Friction **6**(4): 395–406 (2018)
https://doi.org/10.1007/s40544-017-0172-8
ISSN 2223-7690
CN 10-1237/TH
RESEARCH ARTICLE

Friction characteristics of mechanically exfoliated and CVD-grown single-layer MoS_2

Dinh Le Cao KY[1], Bien-Cuong TRAN KHAC[1], Chinh Tam LE[2], Yong Soo KIM[1], Koo-Hyun CHUNG[1,*]

[1] *School of Mechanical Engineering, University of Ulsan, Ulsan 44610, Republic of Korea*

[2] *Department of Physics and Energy Harvest Storage Research Center, University of Ulsan, Ulsan 44610, Republic of Korea*

Received: 17 April 2017 / Revised: 06 June 2017 / Accepted: 07 June 2017

Abstract: In this work, the friction characteristics of single-layer MoS_2 prepared with chemical vapor deposition (CVD) at three different temperatures were quantitatively investigated and compared to those of single-layer MoS_2 prepared using mechanical exfoliation. The surface and crystalline qualities of the MoS_2 specimens were characterized using an optical microscope, atomic force microscope (AFM), and Raman spectroscopy. The surfaces of the MoS_2 specimens were generally flat and smooth. However, the Raman data showed that the crystalline qualities of CVD-grown single-layer MoS_2 at 800 ℃ and 850 ℃ were relatively similar to those of mechanically exfoliated MoS_2 whereas the crystalline quality of the CVD-grown single-layer MoS_2 at 900 ℃ was lower. The CVD-grown single-layer MoS_2 exhibited higher friction than mechanically exfoliated single-layer MoS_2, which might be related to the crystalline imperfections in the CVD-grown MoS_2. In addition, the friction of CVD-grown single-layer MoS_2 increased as the CVD growth temperature increased. In terms of tribological properties, 800 ℃ was the optimal temperature for the CVD process used in this work. Furthermore, it was observed that the friction at the grain boundary was significantly larger than that at the grain, potentially due to defects at the grain boundary. This result indicates that the temperature used during CVD should be optimized considering the grain size to achieve low friction characteristics. The outcomes of this work will be useful for understanding the intrinsic friction characteristics of single-layer MoS_2 and elucidating the feasibility of single-layer MoS_2 as protective or lubricant layers for micro- and nano-devices.

Keywords: atomic force microscope; chemical vapor deposition; grain boundary; friction, mechanical exfoliation; MoS_2

1 Introduction

Atomically thin molybdenum disulfide (MoS_2) exhibits remarkable thermal [1], electrical [2, 3], and optical [4] properties that differ from those of bulk MoS_2. Various electronics [5, 6], optoelectronics [7, 8], and sensors [9, 10] based on atomically thin MoS_2 have been proposed due to these material properties. In addition, the superior mechanical properties [11, 12] and low frictional characteristics [13, 14] of atomically thin MoS_2 suggest that it has potential as an effective protective or lubricant layer [15, 16] for micro- and nano-devices that experience contact sliding during operation.

Recently, the friction characteristics of two-dimensional materials have been extensively investigated using atomic force microscope (AFM). However, most research has focused on graphene [14, 17–21], and the friction characteristics of atomically thin MoS_2 have been reported in only a few studies [14, 22–24]. For example, the friction of atomically thin MoS_2 was found to decrease as the number of layers increased, similar to other two-dimensional materials [14]. This friction behavior was explained based on the puckering

* Corresponding author: Koo-Hyun CHUNG, E-mail: khchung@ulsan.ac.kr

and electron-phonon coupling effects [14, 17]. Friction characteristics of single-layer MoS_2 were also compared to that of single-layer graphene [22]. In addition, the friction characteristics of single-layer MoS_2 deposited on SiO_2, mica, and *h*-BN substrates were investigated. The results showed that friction was the lowest for the *h*-BN substrate, due to a significant reduction in surface roughness [23]. In addition, the friction of single-layer MoS_2 was found to slightly increase with increasing humidity [24]. It was further demonstrated that adding atomically thin MoS_2 to a liquid lubricant can enhance the tribological performances [25]. However, to properly implement atomically thin MoS_2 as a protective or a lubricant layer, more data should be gathered over a wide variety of experimental conditions.

Various methods, such as mechanical exfoliation [9, 26], lithium intercalation-assisted exfoliation [24], liquid exfoliation [27], and physical vapor deposition [28] have been used to prepare atomically thin MoS_2. Thinning using laser-induced ablation [29], thermal annealing [30], and plasma [31] have also been demonstrated for fabricating single-layer MoS_2. However, the lateral size of MoS_2 layers prepared using these methods is often relatively small. In addition, the deposition of MoS_2 with controlled size and shape onto specific locations using these methods is often challenging due to technical difficulties. Chemical vapor deposition (CVD), based on the vapor phase reaction of Mo and S, is one of the most practical methods for large area synthesis [32–35], and hence can be appropriately used to facilitate atomically thin MoS_2 layers as protective or lubricant layers. However, in contrast to the optical [36], electrical [34, 35], and mechanical properties [37], the friction characteristics of CVD-grown MoS_2 have not yet been explored. Considering that CVD-grown MoS_2 can have large variations in grain size, crystalline orientation, and number of defects [32–35], which in turn affect friction characteristics, a systematic approach is needed to fundamentally understand the intrinsic friction characteristics of CVD-grown MoS_2.

In this work, the friction characteristics of single-layer MoS_2 prepared using CVD at various temperatures were systematically investigated using AFM. In particular, given that mechanically exfoliated MoS_2 has high crystallinity with a small number of defects, the friction characteristics of CVD-grown single-layer MoS_2 were compared to those of mechanically exfoliated single-layer MoS_2. The MoS_2 specimens were also characterized using Raman spectra to understand the crystalline qualities of the specimens. The outcomes of this work are expected to aid in evaluating the feasibility of single-layer MoS_2 as protective or lubricant layers for micro- and nano-devices, and optimize CVD growth conditions from a tribological point of view.

2 Experimental details

The MoS_2 specimens were deposited onto a SiO_2/Si substrate using mechanical exfoliation and CVD. The thickness of the thermally grown SiO_2 layer on the Si wafer was about 300 nm. After mechanical exfoliation of the MoS_2 flakes using natural crystalline MoS_2 (SPI supplies), they were carefully examined using an optical microscope to ensure the specimens were free from tape residue. Then, the locations of the single-layer MoS_2 were identified based on the thickness-dependent optical contrast. For the CVD process, MoO_3 (99%, Aldrich) and sulfur powders (99.5%, Alfa) were used as sources of Mo and S, respectively. Crucibles containing MoO_3 and sulfur were placed in the center of a furnace and in the upstream zone of a quartz tube, respectively. The substrates were placed face down above the crucible containing MoO_3. Initially, the quartz tube was pumped down to a base pressure of 60 mTorr and purged with high-purity N_2 gas to eliminate oxygen. Then, the temperature was gradually increased to 400 °C at a rate of 25 °C/min and maintained for 30 min, while the pressure was set to ~700 mTorr with a 100 sccm N_2 gas flow. After the pressure was reduced to atmospheric conditions using 10 sccm N_2 gas flow, the temperature for the reaction was increased to 800 °C, 850 °C, and 900 °C at a rate of 25 °C/min and maintained for 5 min for the growth of single-layer MoS_2 before cooling to room temperature.

After preparation of the MoS_2 specimen, Raman measurements were performed using a confocal Raman system (Alpha300R, Witec) to evaluate the crystalline quality of the MoS_2 layer; the excitation laser with a wavelength of 532 nm was used. For CVD-grown

MoS_2, the isolated flakes were initially formed and then merged into a continuous film during the CVD process. Hence, a laser with a spot size of ~720 nm was carefully focused on isolated MoS_2 flakes to minimize the effects of the grain boundary. In addition, to eliminate laser-induced thermal effects [38, 39] and particle formation [40], the laser power on the specimen surface was limited to below 0.5 mW. The Raman spectra were collected using a 100× objective (NA = 0.9) for 10 s in ambient conditions.

Topographic images of the MoS_2 specimens were obtained using the AFM intermittent contact mode and Si tips with a nominal normal spring constant of 2 N/m (AC240, Olympus). The friction loops were obtained under normal forces ranging from 0 nN to 20 nN using a Si tip with a nominal normal spring constant of 0.2 N/m (PPP-LFM, Nanosensors). For quantitative force measurements using AFM, normal [41] and lateral force [22, 42] calibrations were performed. The force calibration results showed that the normal spring constant and lateral force sensitivity of the Si tip used for friction loop measurements were 0.47 N/m and 5.85 mV/nN, respectively. More than 10 friction loops were obtained at 10 different locations on the specimens under each normal force. In particular, considering that AFM tip wear can readily occur due to contact sliding [43], the friction loops were obtained under increasing and decreasing normal forces to minimize the effects of tip wear on the friction force measurements. In the friction loop measurements, scan distance and sliding speed were set to 300 nm and 375 nm/s, respectively. After the friction loop measurements, friction force images of the grain boundaries of the CVD-grown MoS_2 specimens were obtained to analyze the difference in friction characteristics at the grains and grain boundaries. These friction force images were obtained using the AFM contact mode under 3 nN normal force and 630 nm/s sliding speed.

In addition to friction force measurements, the adhesion forces of the specimens were determined using the force-distance curve [44]. The Si tip used for the friction loop measurements was also used for the force-distance curve measurements. Force-distance curves were obtained before and after the friction loop measurements to further monitor AFM tip wear [45]. More than 10 force-distance curves were obtained at different locations for each specimen. All experiments were performed under ambient conditions (23 ℃ and 35% relative humidity).

3 Results and discussion

Figure 1(a) presents optical microscope images of the mechanically exfoliated single-layer MoS_2 and CVD-grown single-layer MoS_2 at 800 ℃, 850 ℃, and 900 ℃ on the SiO_2/Si substrate. For comparison, optical microscope images of isolated flakes of the CVD-grown MoS_2 are shown in Fig. 1. The shape of the mechanically exfoliated MoS_2 was random with a nominal size of about 10 μm, while the CVD-grown MoS_2 exhibited a triangular shape with different sizes depending on growth temperature. The grain sizes of CVD-grown MoS_2 increased from 5 μm to 15 μm when the temperature increased from 800 ℃ to 850 ℃. However, the grain sizes of CVD-grown MoS_2 significantly decreased, to about 3 μm, at 900 ℃. This grain size dependence on CVD temperature is often noted in the literature. For example, it was demonstrated that the CVD-grown MoS_2 grain size increases when the temperature increases to about 830 ℃, associated with production and diffusion of active mobile species, and then the grain size decreases due to thermal etching when the temperature reaches 900 ℃ [36]. Figure 1(a) indicates that the grain size of CVD-grown MoS_2 at 850 ℃ was the largest, which is consistent with the results from previous research [36].

Considering that surface topography can significantly affect the friction characteristics of two-dimensional materials [20, 23], the MoS_2 specimens were examined using AFM prior to the friction loop measurements. The AFM topographic images of mechanically exfoliated single-layer MoS_2 and CVD-grown single-layer MoS_2 at 800 ℃, 850 ℃, and 900 ℃ obtained with the intermittent contact mode are shown in Fig. 1(b). As shown, the surfaces of the mechanically exfoliated and CVD-grown MoS_2 were generally flat and smooth. However, for the CVD-grown MoS_2 at 800 ℃ and 850 ℃, particles were observed on the substrate surfaces around the flakes. In particular, a large number of particles was observed on the substrate around the CVD-grown MoS_2 flakes at 850 ℃. These particles

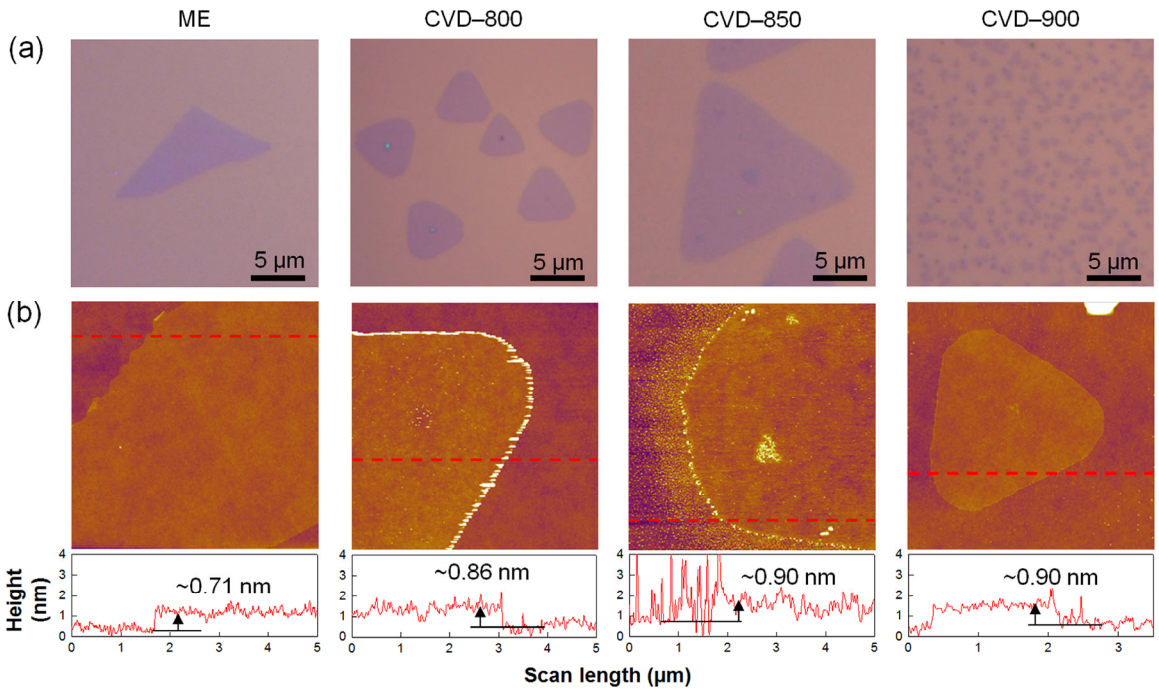

Fig. 1 (a) Optical microscopy and (b) AFM topographic images of mechanically exfoliated single-layer MoS_2 and CVD-grown single-layer MoS_2 at 800 ˚C, 850 ˚C, and 900 ˚C. The red dashed lines indicate the locations of the cross-sectional profiles shown in (b).

could have contained by-products formed during the deposition process. In contrast to the CVD-grown MoS_2 at 800 ˚C and 850 ˚C, the substrate surface around the CVD-grown MoS_2 flakes at 900 ˚C was relatively clean, possibly a result of thermal etching [36]. The surface roughness values of the MoS_2 specimens were determined from AFM topographic images obtained at five different locations within a 500 nm × 500 nm scanning area. The measured surface roughness values of the mechanical exfoliated MoS_2 and CVD-grown MoS_2 at 800 ˚C, 850 ˚C, and 900 ˚C were 0.16 ± 0.01 nm, 0.20 ± 0.01 nm, 0.25 ± 0.01 nm, and 0.16 ± 0.01 nm, respectively. These surface roughness values indicate that the MoS_2 specimens used in this work had flat and smooth surfaces.

The heights of the MoS_2 specimens were determined from the cross-sectional height profiles shown in Fig. 1(b). The height of the MoS_2 prepared using mechanical exfoliation was 0.71 nm. However, the heights of the CVD-grown MoS_2 were slightly larger, ranging from 0.86 nm to 0.90 nm. These values were also larger than the theoretical thickness of single-layer MoS_2 (0.62 nm). These discrepancies between the measured and theoretical thicknesses might have been due to with the presence of adsorbents below the MoS_2 layer, interactions between the MoS_2 layers and substrate [46, 47], and/or AFM measurement uncertainty [48]. Nonetheless, the thicknesses of the single-layer MoS_2 specimens prepared using mechanical exfoliation and CVD were comparable to those of single-layer MoS_2 on a SiO_2/Si substrate.

To understand the crystalline qualities of the MoS_2 specimens, Raman measurements were performed. Figure 2(a) shows examples of the Raman spectra of mechanically exfoliated MoS_2 and CVD-grown MoS_2 at 800 ˚C, 850 ˚C, and 900 ˚C. Two characteristic Raman peaks for MoS_2, E^1_{2g}, and A_{1g}, resulting from the in-plane vibration of Mo-S atoms and out-of-plane vibration of S atoms, respectively [47], are clearly shown in Fig. 2(a). The thickness and crystalline quality of the atomically thin MoS_2 layer can be identified using the frequencies of the E^1_{2g} and A_{1g} peaks and the frequency separation between the two peaks, Δk [32, 47, 49]. The frequencies of the E^1_{2g} and A_{1g} peaks for the mechanically exfoliated and CVD-grown MoS_2 are summarized in Fig. 2(b), along with Δk. The measured value of Δk for the mechanically exfoliated MoS_2 was 17.5 cm^{-1}, which corresponds to single-layer

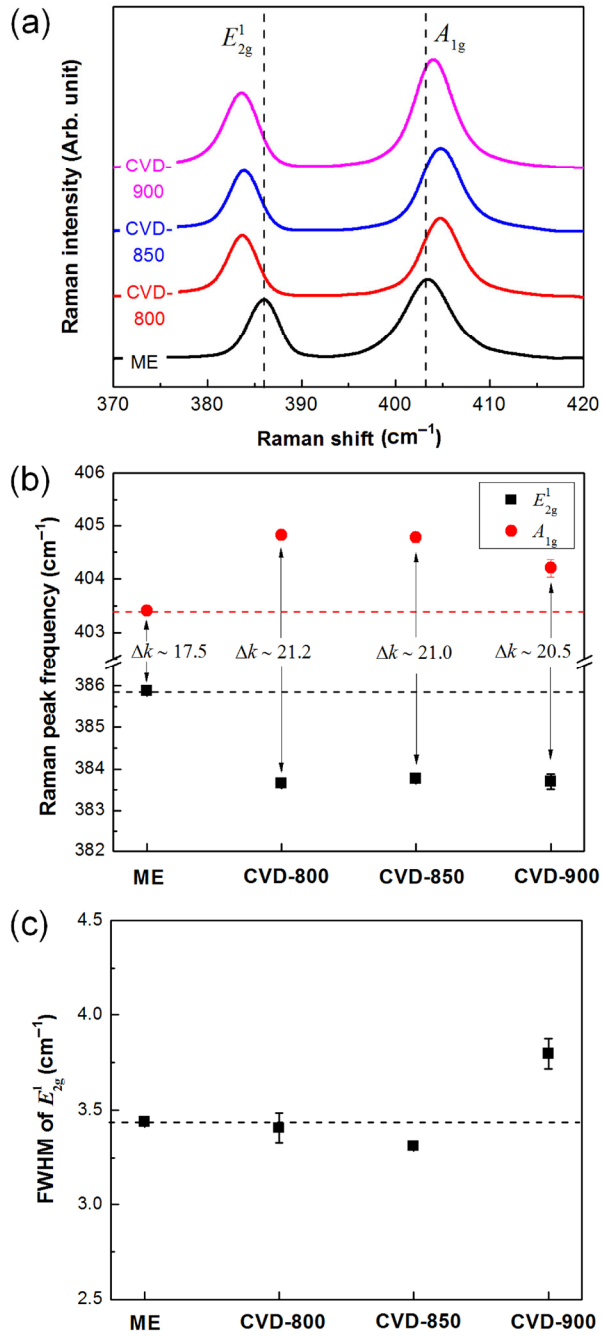

Fig. 2 (a) Raman spectra, (b) frequencies of the E^1_{2g} and A_{1g} peaks and the frequency separation, Δk, and (c) FWHM of the E^1_{2g} peak of the mechanically exfoliated single-layer MoS_2 and CVD-grown single-layer MoS_2 at 800 ℃, 850 ℃, and 900 ℃. In (a), (b), and (c), the frequency of the E^1_{2g} and A_{1g} peaks and FWHM of the E^1_{2g} peak of the mechanically exfoliated single-layer MoS_2 are indicated with dashed lines for comparison. In (b) and (c), the error bar represents one standard deviation.

MoS_2 [47]. Additionally, the measured values of Δk for the CVD-grown MoS_2 at 800 ℃, 850 ℃, and 900 ℃ were 21.2 cm^{-1}, 21.0 cm^{-1}, and 20.5 cm^{-1}, respectively, which agrees with those of CVD-grown single-layer MoS_2 [32, 49]. These Raman measurement results, along with the AFM data shown in Fig. 1(b), show that single-layer MoS_2 formed on the substrate for both the mechanical exfoliation and CVD processes. In addition, the larger values of Δk for the CVD-grown MoS_2 suggest that the CVD-grown MoS_2 may have inferior crystalline qualities compared to the mechanically exfoliated MoS_2 [32, 49].

To further evaluate the crystalline qualities of mechanically exfoliated and CVD-grown MoS_2, the full width at half maximum (FWHM) of the E^1_{2g} peak was also obtained from the Raman data [49], as shown in Fig. 2(c). The FWHM of the E^1_{2g} peaks for the mechanically exfoliated MoS_2 was 3.4 cm^{-1}. Further, as shown, the FWHM of the E^1_{2g} peaks for the CVD grown MoS_2 at 800 ℃ and 850 ℃ agreed with that of the mechanically exfoliated MoS_2. However, the FWHM of the E^1_{2g} peak for the CVD-grown MoS_2 at 900 ℃ was significantly larger than that of the mechanically exfoliated MoS_2. This result further indicates that CVD-grown MoS_2 at 800 ℃ and 850 ℃ have better crystalline qualities than the CVD-grown MoS_2 at 900 ℃ [36, 49].

After characterization of the MoS_2 specimens using an optical microscope, AFM, and Raman spectroscopy, the adhesion and friction characteristics were determined from the force-distance curves and friction loops, respectively. Figure 3 presents examples of the force-distance curves and average adhesion forces between the Si tip used in this work and the MoS_2 specimens, obtained before and after friction loop measurements. As shown in Fig. 3(a), the adhesion forces between the Si tip and CVD-grown MoS_2 at 800 ℃ and 850 ℃ were about 16 nN, which agreed with values found between the Si tip and mechanically exfoliated MoS_2. However, the adhesion force between the Si tip and CVD-grown MoS_2 at 900 ℃ was slightly larger than in the other cases. As shown in Fig. 3(b), the average adhesion forces of mechanically exfoliated single-layer MoS_2 and CVD-grown single-layer MoS_2 at 800 ℃, 850 ℃, and 900 ℃ were 17 ± 2 nN, 16.0 ± 0.3 nN, 16.1 ± 0.7 nN, and 19.8 ± 0.4 nN, respectively. It was hypothesized that interactions with the Si tip might have been enhanced due to imperfections in the crystalline structure, which resulted in a relatively large adhesion force of the CVD-grown single-layer

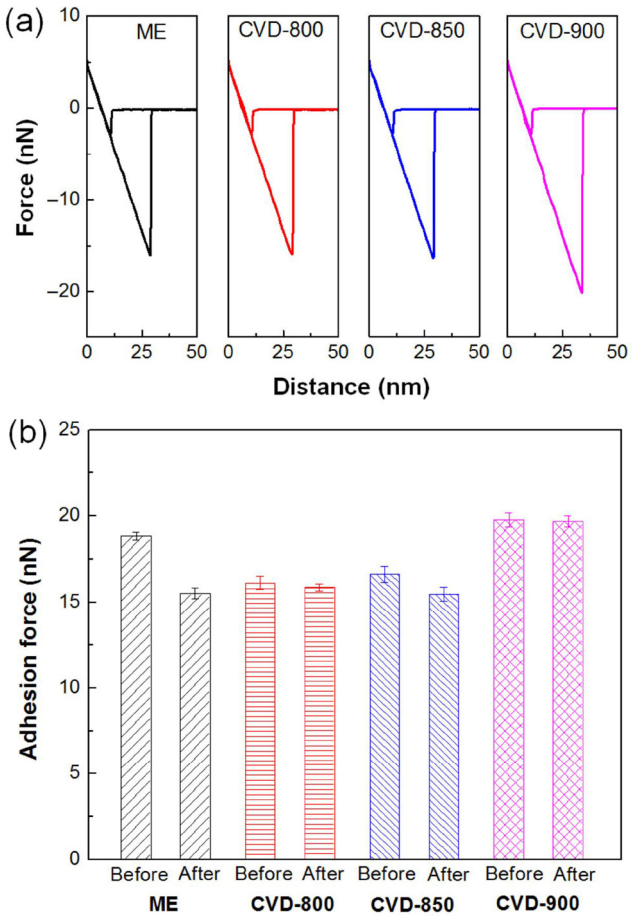

Fig. 3 (a) Examples of force-distance curves and (b) average adhesion forces of the mechanically exfoliated single-layer MoS_2 and CVD-grown single-layer MoS_2 at 800 ℃, 850 ℃, and 900 ℃. In (b), the adhesion forces obtained before and after friction loop measurements are compared. In (b), the error bar represents one standard deviation.

MoS_2 at 900 ℃. In addition, the adhesion force for the mechanically exfoliated MoS_2 slightly decreased after the friction loop measurements. A ripple structure may have been formed due to inhomogeneous interaction between MoS_2 and substrate during mechanical exfoliation, which in turn caused the local differences in frictional and material properties [18, 50]. This local difference in materials properties of the mechanically exfoliated MoS_2 might have caused the difference in adhesion force before and after friction loop measurements, as shown in Fig. 3(b). However, because the CVD-grown MoS_2 may exhibit larger adhesion to the substrate compared to the mechanically exfoliated MoS_2 [51], the effect of ripple structures on the adhesion of CVD-grown MoS_2 was expected to be relatively small. This small effect may be responsible for the good agreement between the adhesion forces of CVD-grown MoS_2 before and after friction loop measurements. In addition, the data shown in Fig. 3 suggests that the tip wear that occurred during friction loop measurements was negligible.

Figure 4(a) shows examples of friction loops for the mechanically exfoliated single-layer MoS_2 and CVD-grown single-layer MoS_2 at 800 ℃, 850 ℃, and 900 ℃ obtained under 10 nN normal force. The friction force of the mechanically exfoliated MoS_2 was about 2 nN under this normal force of 10 nN. However, the friction forces of the CVD-grown MoS_2 were significantly larger than that of the mechanically exfoliated MoS_2, increasing from 3.7 nN to 8.3 nN as temperature increased from 800 ℃ to 900 ℃ with 10 nN of applied normal force.

Variations in the friction force of mechanically exfoliated single-layer MoS_2 and CVD-grown single-layer MoS_2 at 800 ℃, 850 ℃, and 900 ℃ with respect to the normal force are shown in Fig. 4(b). In general, the friction force increased as the normal force increased, as expected. However, a nonlinear relationship between the friction force and normal force [52] was not clearly observed in this work. Figure 4(b) shows that force of the single-layer MoS_2 prepared using mechanical exfoliation increased from 1.5 nN to 2.3 nN when the normal force increased from 0 to 20 nN. As shown, the friction forces of the CVD-grown MoS_2 were significantly larger than those of the mechanically exfoliated MoS_2, which increased with increasing CVD temperature. The friction forces of the CVD-grown MoS_2 at 800 ℃, 850 ℃, and 900 ℃ were, respectively, 2.0, 2.4, and 4.2 times larger than that of the mechanically exfoliated MoS_2. The friction forces under a zero normal force were also the greatest for the CVD-grown MoS_2 at 900 ℃. Furthermore, the increases in friction force with increasing normal force were relatively gradual for the mechanically exfoliated MoS_2 and the CVD-grown MoS_2 at 800 ℃ and 850 ℃, whereas the increase was much more significant for the CVD-grown MoS_2 at 900 ℃.

Many factors, such as the number of layers [14, 17], surface topography [20, 23], interactions with the substrate [21], and crystalline orientation [18] can affect the friction characteristics of two-dimensional materials, in addition to the experimental and environmental conditions [24]. The dependence of

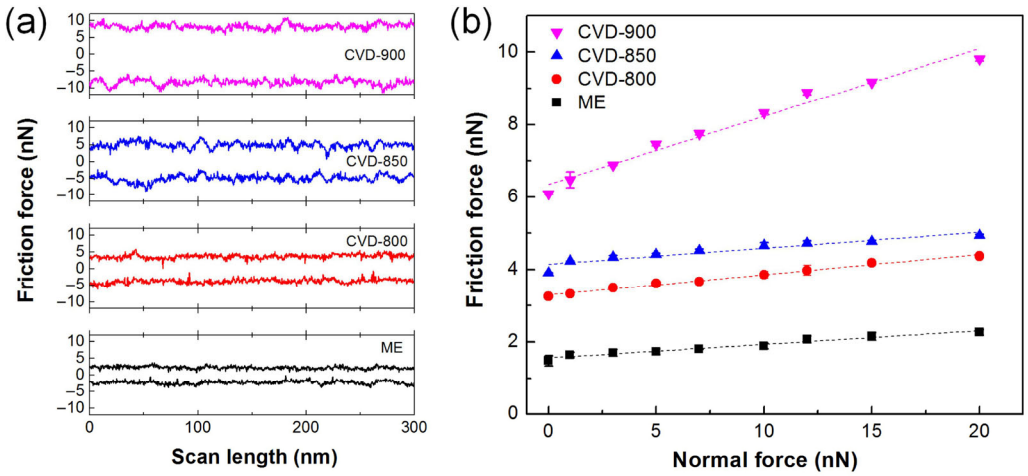

Fig. 4 (a) Examples of friction loops and (b) variations in friction force of the mechanically exfoliated single-layer MoS_2 and CVD-grown single-layer MoS_2 at 800 ˚C, 850 ˚C, and 900 ˚C with respect to the normal force. In (a), the friction loops were obtained under 10 nN normal force. In (b), the dashed lines indicate the linear curve fits and the error bar represents one standard deviation.

MoS_2 friction characteristics on the surface topography is not clearly indicated in Figs. 1 and 4. This lack of correlation might have been due to the surface topographies of the MoS_2 specimens being too homogeneous to affect the friction characteristics. In addition, the effect of crystalline orientation on the friction characteristics was unlikely to appear in the data presented in Fig. 4, considering that the frictional anisotropy due to crystalline orientation is greater at a lower normal force [18]. However, the Raman data in Fig. 2 suggest that the larger friction characteristics of CVD-grown MoS_2 compared to mechanically exfoliated MoS_2 was likely associated with the crystalline imperfections of the CVD-grown MoS_2. The crystalline qualities of CVD-grown MoS_2 at 800 ˚C and 850 ˚C were relatively close to those of the mechanically exfoliated MoS_2. This can explain why the friction characteristics of CVD-grown MoS_2 at 800 ˚C and 850 ˚C were relatively close to those of the mechanically exfoliated MoS_2. However, the crystalline qualities of MoS_2 grown at 900 ˚C were significantly lower than those of the mechanically exfoliated MoS_2, which may be responsible for the relatively high friction characteristics. It should also be noted that the large friction characteristics of the CVD-grown MoS_2 at 900 ˚C may be related to the large adhesion shown in Fig. 3.

The CVD-grown MoS_2 may readily contain grain boundaries because isolated flakes of MoS_2 were merged into a continuous film during the CVD process. Therefore, understanding the friction characteristics at grain boundaries of CVD-grown MoS_2 is important. Figure 5 shows the AFM topographic and friction force images obtained under the intermittent contact and contact modes, respectively, over the grain boundaries of the CVD-grown MoS_2 at 800 ˚C, 850 ˚C, and 900 ˚C. The cross-sectional height profiles and friction loops are also compared in Fig. 5. The friction force images were obtained under 3 nN normal force concurrently with the friction loop. The grain boundaries can be clearly observed in the topographic images. In addition, the cross-sectional height profiles show that the heights at the grain boundaries were slightly larger than those at the grains. The friction force images and friction loops clearly show that the friction forces at the grain boundaries were significantly larger than those at the grains. However, the friction forces on the left and right sides of the grain boundaries were quite similar to each other, indicating that there was an insignificant effect of crystalline orientation on friction of the CVD-grown MoS_2 specimens. The friction forces under 3 nN normal force at the grains and grain boundaries of the CVD-grown MoS_2 at 800 ˚C, 850 ˚C, and 900 ˚C are shown in Fig. 5(c). Compared to the grains, the friction at the grain boundaries increased by factors ranging from 1.5 to 3.0. Defects at the grain boundary may lead to changes in the frictional properties, similar to the

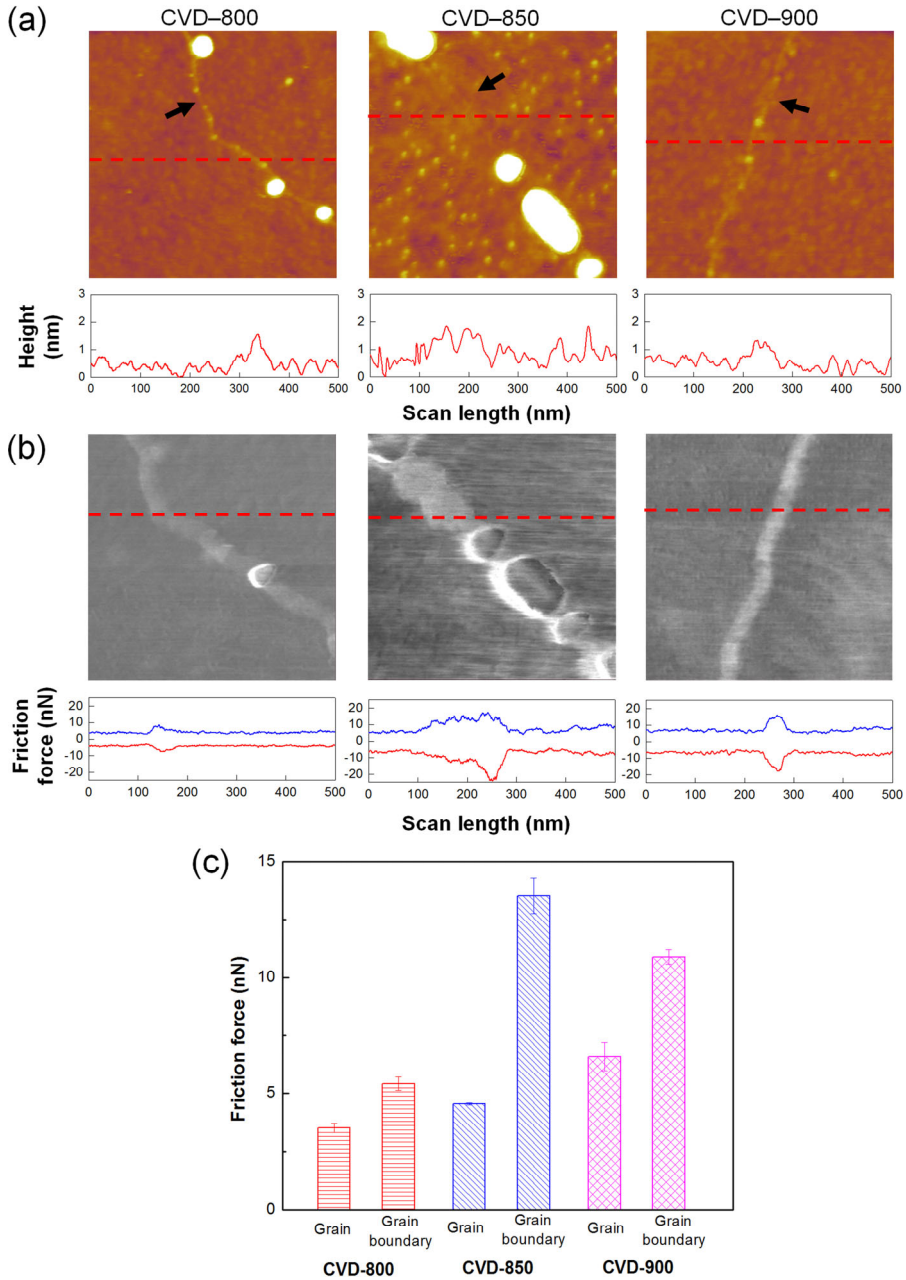

Fig. 5 (a) AFM topographic images and (b) friction force images of the CVD-grown single-layer MoS_2 at 800 ˚C, 850 ˚C, and 900 ˚C, and (c) comparison of the friction forces at the grains and grain boundaries of the CVD-grown MoS_2. The topographic images were obtained with the intermittent contact mode, and the friction force images were obtained using the AFM contact mode under 3 nN normal force. The red dashed lines in (a) and (b) indicate the locations of the cross-sectional height profiles and friction loops, respectively. In (a), the grain boundaries are indicated with black arrows. In (c), the error bar represents one standard deviation.

optical and electrical properties [34, 35]. This outcome suggests that the CVD growth temperature for MoS_2 should also be optimized for grain boundary density to achieve low friction characteristics, considering that CVD growth temperature often affects grain size, as shown in Fig. 1.

According to the experimental results, the CVD-grown single-layer MoS_2 showed greater friction than the mechanically exfoliated single-layer MoS_2, which may be associated with crystalline imperfections in the CVD-grown MoS_2. This outcome indicates that the growth of the single-layer MoS_2, with high

crystalline quality, is preferred when trying to achieve low friction characteristics. The friction force measurement results also suggest that the optimal CVD growth temperature is 800 ℃ based on tribological concerns. However, it should be noted that the frictional properties strongly depend on the test parameters, such as contact pressure, sliding speed, and environmental conditions. In addition, the MoS_2 crystalline structure and quality can be significantly affected by the deposition method and conditions. From this perspective, the results of this work cannot be generalized to all types of single-layer MoS_2. Nevertheless, the outcomes of this work are valid for similar types of MoS_2 grown using the CVD process. Furthermore, the results presented in this work are expected to aid in a more comprehensive and fundamental understanding of the frictional properties of single-layer MoS_2.

4 Conclusions

In this work, the friction characteristics of mechanically exfoliated single-layer MoS_2 and CVD-grown MoS_2 at three different temperatures were systematically investigated using AFM. The mechanically exfoliated and CVD-grown MoS_2 specimens were also examined using an optical microscope, AFM, and Raman spectroscopy to understand the surface characteristics and crystalline qualities of the specimens. The surfaces of the mechanically exfoliated and CVD-grown MoS_2 were generally flat and smooth. The Raman data showed that the crystalline qualities of CVD-grown MoS_2 at 800 ℃ and 850 ℃ were relatively close to those of mechanically exfoliated MoS_2. However, the crystalline qualities of the CVD-grown MoS_2 at 900 ℃ were lower compared to those of the mechanically exfoliated MoS_2. The CVD-grown MoS_2 exhibited greater friction than the mechanically exfoliated single-layer MoS_2, which might have been associated with the crystalline imperfections in CVD-grown MoS_2. In addition, the friction of the CVD-grown MoS_2 increased as the CVD growth temperature increased. In terms of the frictional properties, the optimal growth temperature was 800 ℃ for the CVD process used in this work. Furthermore, the friction at the grain boundaries was larger than at the grain interior by factors of 1.5 to 3.0, which might have been due to defects at the grain boundary. The outcomes of this work are expected to advance the fundamental understanding of intrinsic friction characteristics of single-layer MoS_2, and elucidate the feasibility of single-layer MoS_2 as protective or lubricant layers for micro- and nano-devices.

Acknowledgement

This research was supported by the Basic Science Research Program through the National Research Foundation of Korea (NRF), funded by the Ministry of Science, ICT and Future Planning (NRF-2017R1A2B4009651).

References

[1] Jiang J, Zhuang X, Rabczuk T. Orientation dependent thermal conductance in single-layer MoS_2. *Scientific Reports* **3**: 2209 (2013)

[2] Kuc A, Zibouche N, Heine T. Influence of quantum confinement on the electronic structure of the transition metal sulfide TS2. *Phys Rev B* **83**(24): 245213 (2011)

[3] Wang Q H, Kalantar-Zadeh K, Kis A, Coleman J N, Strano M S. Electronics and optoelectronics of two-dimensional transition metal dichalcogenides. *Nat Nano* **7**(11): 699–712 (2012)

[4] Clark D J, Le C T, Senthilkumar V, Ullah F, Cho H Y, Sim Y, Seong M J, Chung K, Kim Y S, Jang J I. Near bandgap second-order nonlinear optical characteristics of MoS_2 monolayer transferred on transparent substrates. *Appl Phys Lett* **107**(13): 131113 (2015)

[5] Radisavljevic B, Radenovic A, Brivio J, Giacometti V, Kis A. Single-layer MoS_2 transistors. *Nat Nano* **6**(3): 147–150 (2011)

[6] Radisavljevic B, Whitwick M B, Kis A. Integrated circuits and logic operations based on single-layer MoS_2. *ACS Nano* **5**(12): 9934–9938 (2011)

[7] Yin Z, Li H, Li H, Jiang L, Shi Y, Sun Y, Lu G, Zhang Q, Chen X, Zhang H. Single-layer MoS_2 phototransistors. *ACS Nano* **6**(1): 74–80 (2012)

[8] Lee H S, Min S, Chang Y, Park M K, Nam T, Kim H, Kim J H, Ryu S, Im S. MoS_2 nanosheet phototransistors with thickness-modulated optical energy gap. *Nano Lett* **12**(7): 3695–3700 (2012)

[9] Li H, Yin Z, He Q, Li H, Huang X, Lu G, Fam D W H, Tok A I Y, Zhang Q, Zhang H. Fabrication of single- and multilayer MoS_2 film-based field-effect transistors for sensing NO at room temperature. *Small* **8**(1): 63–67 (2012)

[10] Perkins F K, Friedman A L, Cobas E, Campbell P M, Jernigan G G, Jonker B T. Chemical vapor sensing with monolayer MoS_2. *Nano Lett* **13**(2): 668–673 (2013)

[11] Bertolazzi S, Brivio J, Kis A. Stretching and breaking of ultrathin MoS_2. *ACS Nano* **5**(12): 9703–9709 (2011)

[12] Castellanos-Gomez A, Poot M, Steele G A, van der Zant H S J, Agraït N, Rubio-Bollinger G. Elastic properties of freely suspended MoS_2 nanosheets. *Adv Mater* **24**(6): 772–775 (2012)

[13] Martin J M, Donnet C, Le Mogne T, Epicier T. Superlubricity of molybdenum disulphide. *Phys Rev B* **48**(14): 10583–10586 (1993).

[14] Lee C, Li Q, Kalb W, Liu X, Berger H, Carpick R W, Hone J. Frictional characteristics of atomically thin sheets. *Science* **328**(5974): 76–80 (2010)

[15] Donnet C, Erdemir A. Solid lubricant coatings: Recent developments and future trends. *Tribology Letters* **17**(3): 389–397 (2004)

[16] Sen H S, Sahin H, Peeters F M, Durgun E. Monolayers of MoS2 as an oxidation protective nanocoating material. *J Appl Phys* **116**(8): 083508 (2014)

[17] Filleter T, McChesney J L, Bostwick A, Rotenberg E, Emtsev K V, Seyller T, Horn K, Bennewitz R. Friction and dissipation in epitaxial graphene films. *Phys Rev Lett* **102**(8): 086102 (2009)

[18] Choi J S, Kim J, Byun I, Lee D H, Lee M J, Park B H, Lee C, Yoon D, Cheong H, Lee K H, Son Y, Park J Y, Salmeron M. Friction anisotropy–Driven domain imaging on exfoliated monolayer graphene. *Science* **333**(6042): 607–610 (2011)

[19] Kwon S, Ko J, Jeon K, Kim Y, Park J Y. Enhanced nanoscale friction on fluorinated graphene. *Nano Lett* **12**(12): 6043–6048 (2012)

[20] Cho D, Wang L, Kim J, Lee G, Kim E S, Lee S, Lee S Y, Hone J, Lee C. Effect of surface morphology on friction of graphene on various substrates. *Nanoscale* **5**(7): 3063–3069 (2013)

[21] Deng Z, Klimov N N, Solares S D, Li T, Xu H, Cannara R J. Nanoscale interfacial friction and adhesion on supported versus suspended monolayer and multilayer graphene. *Langmuir* **29**(1): 235–243 (2013)

[22] Tran Khac B C, Chung K. Quantitative assessment of contact and non-contact lateral force calibration methods for atomic force microscopy. *Ultramicroscopy* **161**: 41–50 (2016).

[23] Quereda J, Castellanos-Gomez A, Agraït N, Rubio-Bollinger G. Single-layer MoS_2 roughness and sliding friction quenching by interaction with atomically flat substrates. *Appl Phys Lett* **105**(5): 053111 (2014)

[24] Schumacher A, Kruse N, Prins R, Meyer E, Lüthi R, Howald L, Güntherodt H, Scandella L. Influence of humidity on friction measurements of supported MoS_2 single layers. *Journal of Vacuum Science & Technology B* **14**(2): 1264–1267 (1996)

[25] Wu Z, Wang D, Wang Y, Sun A. Preparation and tribological properties of MoS_2 nanosheets. *Advanced Engineering Materials* **12**(6): 534–538 (2010)

[26] Novoselov K S, Geim A K, Morozov S V, Jiang D, Zhang Y, Dubonos S V, Grigorieva I V, Firsov A A. Electric field effect in atomically thin carbon films. *Science* **306**(5696): 666-669 (2004)

[27] Zhou K, Mao N, Wang H, Peng Y, Zhang H. A mixed-solvent strategy for efficient exfoliation of inorganic graphene analogues. *Angewandte Chemie International Edition* **50**(46): 10839–10842 (2011)

[28] Helveg S, Lauritsen J V, Lægsgaard E, Stensgaard I, Nørskov J K, Clausen B S, Topsøe H, Besenbacher F. Atomic-scale structure of single-layer MoS_2 nanoclusters. *Phys Rev Lett* **84**(5): 951–954 (2000).

[29] Castellanos-Gomez A, Barkelid M, Goossens A M, Calado V E, van d Z, Steele G A. Laser-thinning of MoS_2: On demand generation of a single-layer semiconductor. *Nano Lett* 12(6): 3187–3192 (2012)

[30] Lu X, Utama M I B, Zhang J, Zhao Y, Xiong Q. Layer-by-layer thinning of MoS_2 by thermal annealing. *Nanoscale* **5**(19): 8904–8908 (2013)

[31] Liu Y, Nan H, Wu X, Pan W, Wang W, Bai J, Zhao W, Sun L, Wang X, Ni Z. Layer-by-layer thinning of MoS_2 by plasma. *ACS Nano* **7**(5): 4202–4209 (2013)

[32] Zhan Y, Liu Z, Najmaei S, Ajayan P M, Lou J. Large-area vapor-phase growth and characterization of MoS_2 atomic layers on a SiO_2 substrate. *Small* **8**(7): 966–971 (2012)

[33] Lee Y, Zhang X, Zhang W, Chang M, Lin C, Chang K, Yu Y, Wang J T, Chang C, Li L, Lin T. Synthesis of large-area MoS_2 atomic layers with chemical vapor deposition. *Adv Mater* **24**(17): 2320–2325 (2012)

[34] van d Z, Huang P Y, Chenet D A, Berkelbach T C, You Y, Lee G, Heinz T F, Reichman D R, Muller D A, Hone J C. Grains and grain boundaries in highly crystalline monolayer molybdenum disulphide. *Nat Mater* **12**(6): 554–561 (2013)

[35] Najmaei S, Liu Z, Zhou W, Zou X, Shi G, Lei S, Yakobson B I, Idrobo J, Ajayan P M, Lou J. Vapour phase growth and grain boundary structure of molybdenum disulphide atomic layers. *Nat Mater* **12**(8): 754–759 (2013)

[36] Zafar A, Nan H, Zafar Z, Wu Z, Jiang J, You Y, Ni Z. Probing the intrinsic optical quality of CVD grown MoS_2. *Nano Research* **19**(5): 1608–1617 (2016)

[37] Liu K, Yan Q, Chen M, Fan W, Sun Y, Suh J, Fu D, Lee S, Zhou J, Tongay S, Ji J, Neaton J B, Wu J. Elastic properties of chemical-vapor-deposited monolayer MoS_2, WS_2, and their bilayer heterostructures. *Nano Lett* **14**(9): 5097–5103 (2014)

[38] Najmaei S, Liu Z, Ajayan P M, Lou J. Thermal effects on the characteristic raman spectrum of molybdenum disulfide (MoS_2) of varying thicknesses. *Appl Phys Lett* **100**(1): 013106 (2012)

[39] Lanzillo N A, Glen Birdwell A, Amani M, Crowne F J, Shah P B, Najmaei S, Liu Z, Ajayan P M, Lou J, Dubey M, Nayak S K, O'Regan T P. Temperature-dependent phonon shifts in monolayer MoS_2. *Appl Phys Lett* **103**(9): 093102 (2013)

[40] Tran Khac B C, Jeon K, Choi S T, Kim Y S, DelRio F W, Chung K. Laser-induced particle adsorption on atomically thin MoS_2. *ACS Appl Mater Interfaces* **8**(5): 2974–2984 (2016)

[41] Hutter J L, Bechhoefer J. Calibration of atomic-force microscope tips. *Rev Sci Instrum* 64(7): 1868–1873 (1993)

[42] Varenberg M, Etsion I, Halperin G. An improved wedge calibration method for lateral force in atomic force microscopy. *Rev Sci Instrum* **74**(7): 3362–3367 (2003)

[43] Chung K H. Wear characteristics of atomic force microscopy tips: A reivew. *International Journal of Precision Engineering and Manufacturing* **15**(10): 2219–2230 (2014)

[44] Cappella B, Dietler G. Force-distance curves by atomic force microscopy. *Surface Science Reports* **34**(1–3): 1–104 (1999)

[45] Gotsmann B, Lantz M A. Atomistic wear in a single asperity sliding contact. *Phys Rev Lett* **101**: 125501 (2008)

[46] Lee C, Yan H, Brus L E, Heinz T F, Hone J, Ryu S. Anomalous lattice vibrations of single- and few-layer MoS_2. *ACS Nano* **4**(5): 2695–2700 (2010).

[47] Li H, Zhang Q, Yap C C R, Tay B K, Edwin T H T, Olivier A, Baillargeat D. From bulk to monolayer MoS_2: Evolution of raman scattering. *Advanced Functional Materials* **22**(7): 1385–1390 (2012)

[48] Nemes-Incze P, Osváth Z, Kamarás K, Biró L P. Anomalies in thickness measurements of graphene and few layer graphite crystals by tapping mode atomic force microscopy. *Carbon* **46**(11): 1435–1442 (2008)

[49] Yu Y, Li C, Liu Y, Su L, Zhang Y, Cao L. Controlled scalable synthesis of uniform, high-quality monolayer and few-layer MoS2 films. *Scientific Reports* **3**: 1866 (2013)

[50] Brivio J, Alexander D T L, Kis A. Ripples and layers in ultrathin MoS_2 membranes. *Nano Lett* **11**(12): 5148–5153 (2011)

[51] Plechinger G, Mann J, Preciado E, Barroso D, Nguyen A, Eroms J, SchÃller C, Bartels L, Korn T. A direct comparison of CVD-grown and exfoliated MoS_2 using optical spectroscopy. *Semiconductor Science and Technology* **29**(6): 064008 (2014).

[52] Mo Y, Turner K T, Szlufarska I. Friction laws at the nanoscale. *Nature* **457**(7233): 1116–1119 (2009)

Dinh Le Cao KY. He received his M.S. degree in mechanical engineering in 2010 from University of Technology, Ho Chi Minh City, Vietnam. He is currently pursuing his PhD degree in the Tribology and Surface Engineering Laboratory at University of Ulsan, Republic of Korea. His research interests include fundamental understanding of friction characteristics of nanomaterials from experiments and molecular dynamics simulation.

Bien-Cuong TRAN KHAC. He received his M.S. degree in mechanical engineering in 2014 from University of Ulsan, Republic of Korea. He is currently pursuing his PhD degree in the Tribology and Surface Engineering Laboratory at the same university. His research interests include tribology and surface damage characteristics of atomically thin (2D) materials.

Chinh Tam LE. He received his B.S. degree in material science in 2012 from Ho Chi Minh University of Natural Science in Vietnam. After then, he joined the Semiconductor Device Research Laboratory from 2013 and is currently the PhD student in University of Ulsan, Republic of Korea. His interest research is synthesis and optical characterization of monolayer transition metal dichalcogenides MX2.

Yong Soo KIM. He received his M.S. and PhD degrees in physics from Seoul National University, Republic of Korea in 1993 and 1998, respectively. After then, he was a senior and principle researcher at R&D division, SK-Hynix Inc. He joined the Department of Physics at University of Ulsan, South Korea from 2008. His current position is associate professor, chair of physics department and director of human resource center for novel materials research experts (BK21+ program). His research interest includes organic-inorganic hybrid solar cell, 2-D layer materials relating optoelectronic device, especially transitional metal dichalcogenide growth and its optical characteristics.

Koo-Hyun CHUNG. He received his M.S. and PhD degrees in mechanical engineering from Yonsei University, Republic of Korea, in 1997 and 2005, respectively. His current position is an associate professor at the School of Mechanical Engineering, University of Ulsan, South Korea. His research areas cover tribology, micro/nano tribology, adhesion, surface engineering, molecular dynamics simulation, as well as themes relating to material science.